Kinetics and Catalysis, Vol. 46, No. 2, 2005, pp. 269–281. Translated from Kinetika i Kataliz, Vol. 46, No. 2, 2005, pp. 288–301.

Activation of the C–O Bond on the Surface of Palladium: An *In situ* Study by X-ray Photoelectron Spectroscopy and Sum Frequency Generation

V. V. Kaichev*, V. I. Bukhtiyarov*, G. Rupprechter, and H.-J. Freund****

** Boreskov Institute of Catalysis, Siberian Division, Russian Academy of Sciences, Novosibirsk, 630090 Russia*

*** Fritz Haber Institute der MPG, D-14195 Berlin, Germany*

Received February 27, 2004

Abstract—An *in situ* study of the adsorption of CO on atomically smooth and defect Pd(111) surfaces was performed over wide ranges of temperatures (200–400 K) and pressures (10^{-6}–1 mbar) by X-ray photoelectron spectroscopy and sum frequency generation. Both of the techniques indicated that CO was adsorbed as three-fold hollow, bridging, and terminal species to form well-known ordered structures on the surface. In the course of the *in situ* experiments, no signs of CO dissociation or of the formation of carbonyl structures ($Pd(CO)_n$, $n > 1$) were detected. The mechanism of C–O bond activation in the course of methanol decomposition on the surface of palladium was considered. It was found that the adsorption of methanol on the surface of palladium essentially depends on pressure. Along with the well-known reaction path of methanol dehydrogenation to CO and hydrogen, a slow process of methanol decomposition with C–O bond cleavage was observed at elevated pressures. In this case, the formation of carbon deposits finally resulted in the carbonization and complete deactivation of the surface. A mechanism for C–O bond activation on the surface of palladium was proposed; the geometry of adsorption complexes plays an important role in this mechanism.

INTRODUCTION

The mechanism of activation of the C–O bond on the surfaces of transition metals has attracted considerable attention from researchers in the area of heterogeneous catalysis. This is primarily due to studies on the reaction mechanisms of carbon monoxide hydrogenation or methanol oxidation and dehydrogenation, which form the basis of the commercial manufacture of hydrocarbons, aldehydes, alcohols, hydrogen, etc. [1–7]. Thus, for example, the activation (cleavage) of the C–O bond is a necessary condition for the synthesis of hydrocarbons (Fischer-Tropsch process). At the same time, the formation of carbon as a result of CO dissociation can be responsible for loss in catalytic activity due to the blocking of active centers on the catalyst surface. Actually, the activation of the C–O bond depending on the nature of the catalyst, the composition of reactants, and reaction conditions is responsible for the activity and selectivity of the above reactions. From this standpoint, a detailed study of the mechanism of activation of the C–O bond on the surfaces of transition metals is undoubtedly favorable for the prediction of catalytic effects and, correspondingly, for the development of more effective catalysts for a particular reaction.

A large body of scientific research in this area was devoted to the adsorption of simple molecules (CO, CH_3OH, etc.) on metal surfaces under ultrahigh-vacuum (UHV) conditions. The use of currently available physical techniques for studying the surface of well-characterized model samples (single crystals, foils, supported metal clusters, etc.) provides an opportunity to perform controllable (in terms of composition, structure, and purity) and reproducible experiments. Individual elementary steps of catalytic reactions can be studied on the atomic and molecular level. At the same time, the majority of these data cannot be directly used in the area of applied catalysis, mainly because of the so-called "pressure gap" problem. Indeed, under conditions of surface science experiments ($P < 10^{-6}$ mbar, 1 mbar = 0.75 Torr), the concentrations of reaction intermediates and the rates of individual steps of a catalytic reaction can be much lower than the sensitivity threshold of physical techniques being used. Consequently, information obtained in this case is not always representative of to the chemical processes that occur on the surface of an actually operating catalyst ($P > 10^3$ mbar).

To solve this problem, many attempts have been made in recent years to develop new methods or modernize known methods for surface studies. The aim of these studies was to perform *in situ* experiments (i.e., directly in the course of a reaction) [8–22]. Reflectance–absorption IR spectroscopy [8–10], including IR spectroscopy in a polarization modulation mode [9, 10]; sum frequency generation (SFG) spectroscopy [11–15]; X-ray absorption edge spectroscopy [16–18]; and X-ray photoelectron spectroscopy (XPS) [19–22] are among the methods that can be effective at pressures close to those in actual catalysis ($P > 0.1$ mbar).

In this work, we demonstrated the advantages of a combined use of XPS and SFG spectroscopic tech-

0023-1584/05/4602-0269 © 2005 MAIK "Nauka/Interperiodica"

niques in an *in situ* study of model catalytic systems. XPS is an element-sensitive technique for surface analysis; it yields direct quantitative information on the chemical composition of an adsorption layer. A specially designed photoelectron spectrometer used in this study allowed us to perform experiments at pressures up to 0.5 mbar, which is higher than that in commercial models by five orders of magnitude. SFG upon the exposure of a test surface to radiation from two pulsed lasers with wavelengths in the visible and IR regions of the spectrum is a sophisticated technique. At the same time, this is one of the most promising optical techniques for *in situ* studies of the nature of adsorption complexes [11–15]. The physical fundamentals of this technique have been described in sufficient detail [14, 23–25]. In the course of experiments, the laser radiation frequency in the visible region remained constant (λ = 532 nm), whereas the frequency of the IR laser varied within certain limits. This allowed us to study vibrational SFG "resonances" directly related to vibrational excitation of adsorbed molecules [11–15]. In accordance with selection rules, vibrations active in both IR and Raman spectroscopy manifest themselves in SFG spectra. An evident advantage of this technique consists in the possibility of obtaining the vibrational spectra of adsorbates at elevated pressures (up to atmospheric pressure) under *in situ* conditions.

The aim of this work was to study the interactions of CO and methanol with the surface of palladium over wide ranges of temperatures and pressures with the use of XPS and SFG techniques.

EXPERIMENTAL

Experiments with the use of vibrational spectroscopy (SFG) were performed on a specially designed UHV spectrometer [14, 15]. The spectrometer had two levels: an UHV chamber for sample preparation as the top level and a high-pressure cell for *in situ* experiments as the bottom level. The pressure of residual gases in the system was no higher than 5×10^{-10} mbar. The preparation chamber was designed for the precleaning and characterization of samples by temperature-programmed desorption (TPD), Auger spectroscopy, and low-energy electron diffraction (LEED). The high-pressure cell was a stainless-steel cylinder with optical windows for laser radiation input and output and a system for independent evacuation and gas admission [14]. Simultaneously to the recording of SFG spectra, the composition of a reaction mixture in the cell could be analyzed by a gas chromatograph. Correspondingly, the accumulation of products in the course of catalytic reactions could be monitored in a batch mode.

The XPS experiments were performed on a VG ESCALAB HP UHV spectrometer. The design and main performance characteristics of this spectrometer were described in detail previously [17, 19–22]. The vacuum system consisted of an analytical chamber and two preparation chambers; both of them had an independent evacuation facility and a gas admission system. The pressure of residual gases was no higher than 5×10^{-10} mbar. A distinctive feature of the spectrometer is the presence of systems for the differential evacuation of an X-ray source and an analyzer of the kinetic energies of electrons. With the use of a high-pressure cell embedded in the analytical chamber of the spectrometer, this provides an opportunity to record XPS spectra *in situ* at pressures up to 0.5 mbar under flow conditions [19–22]. The gas flow rate over the sample and the composition of the reaction mixture were adjusted with precision inlet needle valves. A thermoresistive sensor was used for pressure measurements within the catalytic cell.

The XPS spectra were measured with the use of characteristic AlK_α radiation ($h\nu$ = 1486.6 eV). The scale of binding energies (E_b) of the spectrometer was calibrated using the position of the Pd $3d_{5/2}$ line (E_b = 334.9 eV) in the spectrum of the clean Pd(111) surface. To obtain detailed information, the spectra were decomposed into individual components. After background subtraction by the Shirley method, the experimental curve was decomposed into a number of lines corresponding to the photoemission of electrons from the inner levels of atoms in different chemical environments. The peak contours were approximated by a symmetric Doniach–Sunjic function. The line intensities in the spectra were normalized to the integrated intensity of the corresponding Pd 3*d* lines.

A rectangular Pd(111) single crystal of size 10×5 mm and 1.5 mm in thickness, which was prepared in accordance with the standard procedure, was used as a test material in the experiments. A resistive heater (W or Mo wire) was fixed directly to the lateral surfaces of the sample. A Chromel–Alumel thermocouple, which was spot-welded to the edge of the crystal, was used for temperature monitoring. A cooling system with liquid nitrogen was used for operations at low temperatures. Before experiments, the palladium surface was cleaned in the vacuum chamber of the spectrometer using a cycle of treatments including etching with 1- to 2-keV argon ions, vacuum heating to 1250 K followed by rapid cooling in oxygen ($P = 10^{-6}$ mbar) to 600 K, and rapid heating in a vacuum to 1250 K. No impurities were detected on the surface of palladium after several treatment cycles; according to LEED data, the surface structure corresponded to the (111) face. The purity of the surface was monitored by XPS and Auger spectroscopy.

Special attention was focused on the purity of gases used in this study. It is well known that carbon monoxide readily reacts with transition metals to form volatile carbonyl compounds [26, 27]. Therefore, CO contained considerable amounts of iron carbonyl and nickel carbonyl impurities after long-term storage in metal gas cylinders [15, 21]. These compounds are unstable, and they readily dissociate at the surface of palladium even at room temperature [28]. As a result, the decomposi-

tion products of carbonyl compounds can be accumulated on the surface of test samples, in particular, in the experiments performed at elevated pressures. In turn, this may result in the inadequate interpretation of experimental data. To eliminate the above problems, the gas cylinder containing carbon monoxide was cooled to liquid nitrogen temperature in the course of all of the experiments. In this case, the partial pressure of carbonyls in a gas phase was negligibly low, and the accumulation of foreign impurities (C, Fe, Ni, etc.) on the surface of palladium was not detected for several hours. Before being supplied to the chamber of the spectrometer, methanol was purified by freezing and pumping to an ultrahigh vacuum. The purity of gases supplied to the cell was monitored with the use of a quadrupole mass spectrometer.

RESULTS AND DISCUSSION

Adsorption of CO on the Pd(111) Surface

The great interest of the adsorption of CO on the surface of palladium to researchers is due to the practical importance of this metal (palladium is a constituent of automotive exhaust afterburning catalysts) and the sensitivity of the spectral characteristics of CO_{ads} to the structure of surface centers. The latter circumstance is responsible for the use of CO as a test molecule. It was found in many studies that the adsorption of CO on the surface of palladium under UHV conditions is nondissociative; that is, it occurs without C–O bond cleavage [8–10, 13–15, 21, 29–38]. The initial sticking coefficient is close to unity [31]. The adsorption is reversible; carbon monoxide is completely removed from the surface at ~500 K. The CO molecule is bound to the metal surface through the carbon atom, and the molecular axis is oriented perpendicularly to the surface. Depending on the surface structure and coverage, CO is adsorbed to form 1-, 2-, and 3-fold bound states. The higher the coordination of CO, the stronger the bond of CO with the surface.

The combined use of LEED and vibrational spectroscopy demonstrated that the frequencies of stretching vibrations of the C–O bond in carbon monoxide molecules adsorbed in 3-, 2-, and 1-fold bound states on the Pd(111) surface are 1850, 1950, and 2100 cm^{-1}, respectively [30–35]. At low surface coverages, lower than 0.33 monolayer (ML) (1 ML corresponds to the density of atoms in the surface layer of the Pd(111) face and is equal to 1.53×10^{15} atom/cm^2), CO was adsorbed in a threefold hollow bound state to form the $(\sqrt{3} \times \sqrt{3})$R30°–1CO structure. In this case, an absorption band at ~1850 cm^{-1} was observed in the IR-spectral region of stretching vibrations ν(C–O) [31]. A further increase in the surface concentration of CO resulted in the population of twofold bound states and in the formation of the $c(4 \times 2)$–2CO structure at the coverage $\Theta = 0.5$ ML. In this case, an absorption band observed at ~1920 cm^{-1} corresponded to the stretching vibrations of CO in a bridging position (the CO molecule bound to two palladium atoms) [31]. At high coverages, CO molecules are adsorbed in bridging and terminal (singly bound) states to form, for example, the $(4\sqrt{3} \times 8)$rect structure at $\Theta = 0.63$ ML. The maximum CO coverage for the Pd(111) face is 0.75 ML and corresponds to the (2×2)–3CO structure (two molecules adsorbed in a threefold hollow and one in a terminal state). In this case, two intense lines at 1895 and 2107 cm^{-1} were observed in the IR spectrum of ν(C–O) stretching vibrations [13, 15, 30–33]. In the case of UHV experiments, an increase in the surface coverage with adsorbed CO was provided by a decrease in the temperature (a maximum coverage was reached at T_{ads} = 100 K).

At elevated pressures, the adsorption of CO on the single-crystal surfaces of palladium occurred with the formation of the same ordered structures as under UHV conditions. Figure 1 shows the SFG and XPS spectra measured *in situ* in the course of CO adsorption on the atomically smooth surface of a Pd(111) single crystal at 400 K. At a low pressure ($P_{CO} = 10^{-6}$ mbar), the SFG spectrum exhibited a line at 1910 cm^{-1}, which corresponds to the stretching vibrations of CO molecules adsorbed in a bridging state. In the corresponding C 1*s* spectrum (Fig. 1b), a narrow symmetrical line appeared at 285.6 eV. In accordance with SFG data, this line can be attributed to CO molecules adsorbed in a bridging state. As the pressure was increased, an SFG resonance in the region 2075–2080 cm^{-1} was observed; this suggests the appearance of terminal states because of an increase in the surface concentration of CO. The C 1*s* line in the XPS spectrum broadened with increasing pressure, and an additional signal with E_b = 286.3 eV due to the terminal states of CO could be distinguished by the deconvolution of the spectrum into individual components. This assignment of C 1*s* signals was supported by data published by Surnev *et al.* [36], who found using high-resolution XPS that CO molecules adsorbed on the Pd(111) surface in 3-, 2-, and 1-fold bound states are characterized by similar C 1*s* binding energies of 285.6 ± 0.1, 285.85, and 286.3 eV, respectively. The C 1*s* line at 290 eV, which appeared at high pressures (Fig. 1b, curve *3*), corresponds to carbon monoxide in the gas phase; as a rule, this line was observed at a CO pressure higher than 5×10^{-2} mbar [21].

Note that not only XPS but also SFG spectroscopy yields quantitative information on the surface coverage with CO [21]. In the case of XPS, the integrated intensity of the C 1*s* XPS line is directly proportional to the surface concentration of CO, whereas quantitative information in the case of SFG spectroscopy can be obtained from an analysis of the positions of the resonance lines observed. This follows from the fact that the frequency of stretching vibrations ν(C–O) depends on lateral interactions in the adsorption layer. As the number of CO molecules on the surface of palladium was

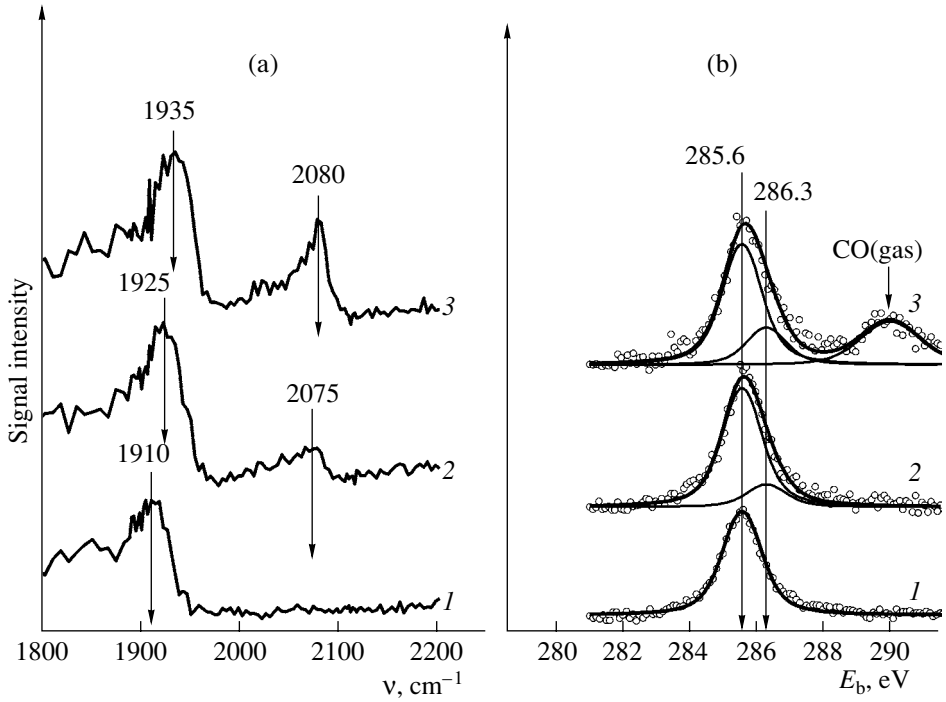

Fig. 1. (a) SFG and (b) C 1*s* XPS spectra recorded *in situ* in the course of CO adsorption on the atomically smooth surface Pd(111) at 400 K and P_{CO}, mbar: (a) (*1*) 10^{-6}, (*2*) 10^{-3}, and (*3*) 1; (b) (*1*) 10^{-6}, (*2*) 5×10^{-3}, and (*3*) 0.1.

decreased, the dipole–dipole interaction of CO molecules in the adsorption layer weakened and the competition of these molecules for the *d* electrons of the metal decreased. As a result, a low-frequency shift of ν(C–O) bands due to stretching vibrations occurred. Correspondingly, each of the well-known structures of adsorbed CO exhibited a characteristic IR spectrum [30–35, 38]. Table 1 and Fig. 2 summarize the results of quantitative analysis.

As can be seen, the surface coverage of Pd(111) with CO molecules depends on temperature and pressure. The maximum coverage Θ = 0.75 ML was reached at 200 K and 1 mbar [15]. An increase in the temperature noticeably decreased the equilibrium concentration of CO. At 400 K, the surface coverage with CO was as low as 0.55 ML even at ~1 mbar. The above results are consistent with published data [8–10, 31]. Thus, on the Pd(111) surface at 100 K, the formation of the (2 × 2) structure was observed at a pressure of 10^{-6} mbar, whereas 700 mbar was required for the surface coverage Θ = 0.75 ML even at 300 K [15]. The isosteric heat of CO adsorption was ~23 kcal/mol at Θ = 0.5 ML, as estimated based on the above data from the Clausius–Clapeyron equation ($d(\ln P)/d(1/T) = -E/R$). This value is consistent with the results of thermal desorption studies [29, 32, 34].

Therefore, we used both high pressures and low temperatures to reach maximum CO coverage. Figure 3 shows SFG and XPS spectra measured *in situ* in the course of CO adsorption on the atomically smooth surface of a Pd(111) single crystal at 200 K and P_{CO} = 1 (SFG) or

Table 1. Quantitative data on the coverage (Θ, ML) of the atomically smooth surface Pd(111) with CO depending on temperature and pressure

XPS				SFG			
P, mbar	200 K	300 K	400 K	*P*, mbar	200 K	300 K	400 K
1×10^{-6}	0.66	0.50	0.36	1×10^{-6}	0.65	0.50	0.45
5×10^{-3}	0.71	0.53	0.48	1×10^{-3}	0.70	0.55	0.50
1×10^{-1}	0.71	0.63	0.54	1	0.75	0.60	0.55

Note: To obtain the absolute values of surface coverage from XPS data, the coverage Θ = 0.50 ML was used as a reference point ($P = 10^{-6}$ mbar, T = 300 K [31, 38]). In the case of SFG, the coverage (±0.05 ML) was evaluated based on the dependence of the vibrational frequency ν(C–O) on the surface concentration of CO. The SFG spectra of ordered structures at the coverages Θ = 0.50, 0.63, and 0.75 ML were used as reference points [15, 21, 31, 38].

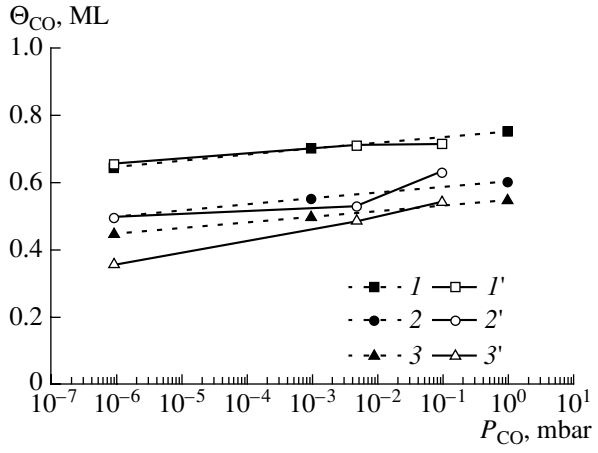

Fig. 2. The pressure dependence of the equilibrium CO coverage on the surface Pd(111) at temperatures of (*1*, *1*') 200, (*2*, *2*') 300, and (*3*, *3*') 400 K from (*1–3*) XPS and (*1*'–*3*') SFG data.

0.1 (C 1*s*) mbar. In accordance with published data, the SFG spectrum under these conditions exhibited bands due to CO molecules adsorbed in threefold hollow and terminal states. In Fig. 3b, the corresponding C 1*s* spectrum is compared with the spectrum obtained at T = 400 K and $P_{CO} = 10^{-6}$ mbar, that is, under conditions of the complete absence of a terminal state (see Fig. 1a). In our opinion, difference spectrum *3*, which was obtained by subtracting the spectrum of the threefold hollow state from the total spectrum, belongs to only the terminal (on-top) state of adsorbed CO. An additional support for the validity of this assignment consists in the ratio between the surface concentrations of threefold bound CO_{ads} species obtained from the spectrum measured at 10^{-6} mbar and 400 K and the difference spectrum; this ratio was found to be equal to ~1.9. The resulting value is consistent with a ratio of 2, which was determined previously for the (2 × 2)–3CO structure, which characterizes maximum CO coverage (Θ = 0.75 ML). Note that a clearly defined component due to the terminal state of adsorbed CO in the C 1*s* spectrum (E_b = 286.3 eV) lends support to the validity of the procedure of deconvolution used in the analysis of spectra in Fig. 1.

Note that, in the course of *in situ* experiments performed in pressure and temperature ranges from 10^{-6} to 1 mbar and from 200 to 400 K, respectively, we failed to detect CO dissociation traces or the formation of new adsorption states on the surface of Pd(111). In the case of CO dissociation or the formation of carbonyl structures (for example, $Pd(CO)_2$), the appearance of additional photoemission signals at 284 or 287 eV, respectively, would be expected [39, 40]. In contrast, data indicative of the dissociative character of CO adsorption on the surface of fine palladium particles were reported in a number of publications [41–46]. Stará and Matolín [46] reached a conclusion indicating the dissociation of CO on palladium particles smaller than 4 nm. The resulting carbon blocked the surface and prevented

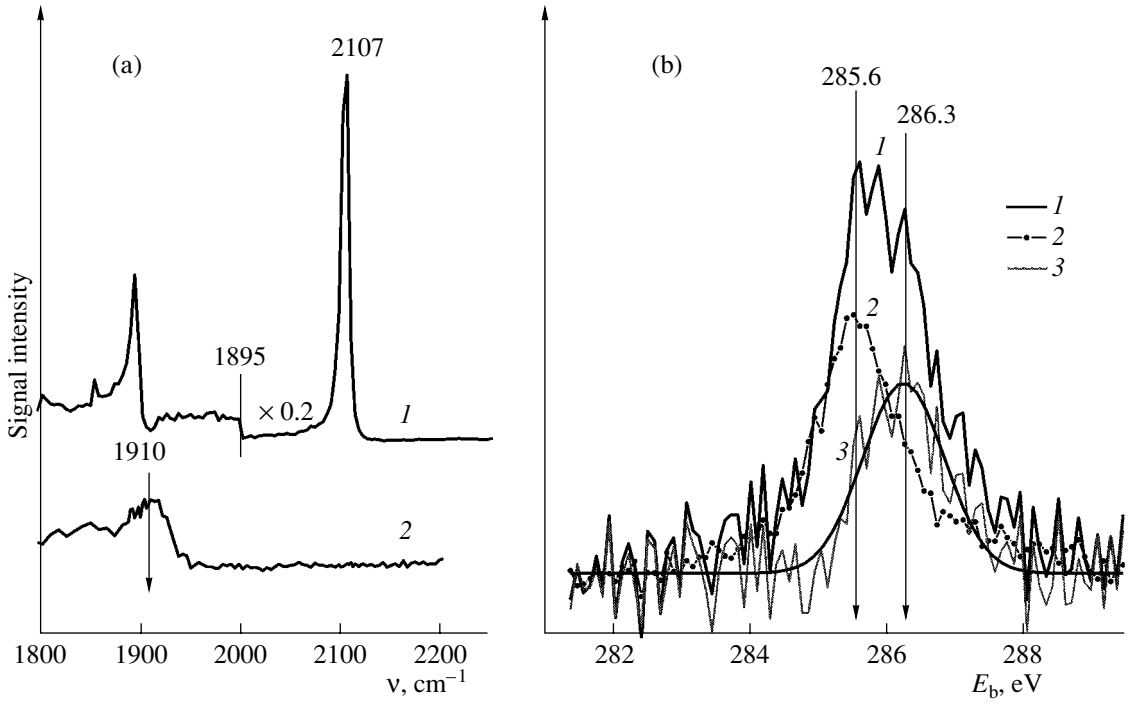

Fig. 3. (a) SFG and (b) C 1*s* XPS spectra recorded *in situ* in the course of CO adsorption on the atomically smooth surface Pd(111) at temperatures of (*1*) 200 and (*2*) 400 K and P_{CO}, mbar: (a) (*1*) 1 or (*2*) 10^{-6}; (b) (*1*) 0.1 and (*2*) 10^{-6}. Spectrum *3* was obtained by the direct subtraction of spectrum *2* from spectrum *1*.

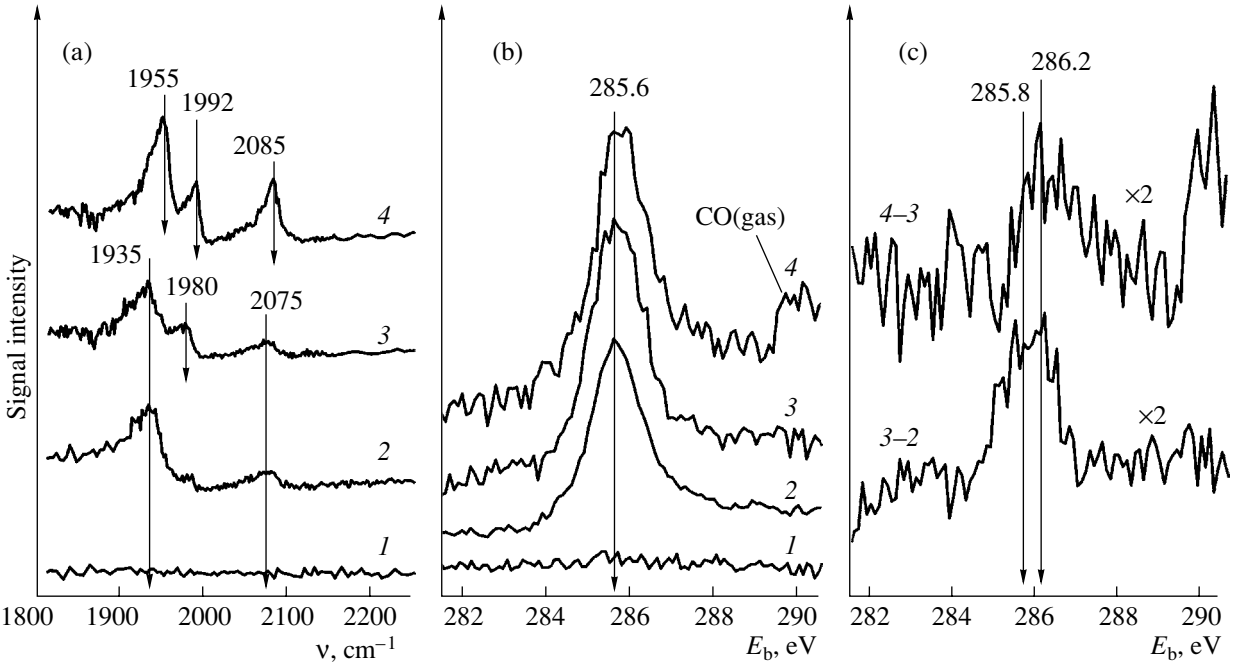

Fig. 4. (a) SFG and (b) C 1*s* XPS spectra recorded *in situ* in the course of CO adsorption at 300 K on the (*1*, *2*) atomically smooth and (*3*, *4*) defect surfaces Pd(111) at P_{CO}, mbar: (a) (*1*) <10^{-10} and (*2*, *3*) 10^{-6}; (b) (*1*) <10^{-10}, (*2*, *3*) 10^{-6}, and (*4*) 10^{-1}. (c) Difference spectra *3–2* and *4–3* were obtained by the direct subtraction of corresponding XPS spectra.

subsequent adsorption of CO. The rate of CO decomposition increased with decreasing particle size. The partial decomposition of carbon monoxide on the surface of supported palladium particles of size 2–3 nm was observed even at low pressures of CO [44–46].

According to Matolín and coauthors [44–46], the disproportionation of carbon monoxide on the surface of fine palladium particles is directly related to the appearance of specific surface defects. It is believed that this conclusion is supported by the results obtained by Matolín *et al.* [47]. In the cited study, the dissociation of CO and the formation of elemental carbon at 410 K and $P_{CO} = 10^{-6}$ mbar occurred on the surface of palladium foil subjected to ion bombardment. Well-annealed foil was inactive in the disproportionation of CO under the same conditions.

Note that CO dissociation on the surface of palladium particles of size 2–3 nm was not detected in other studies [48–52]. An explanation of this contradiction is the effect of catalyst preparation procedures on the shape of supported palladium particles. It was hypothesized that the morphology of particles and, correspondingly, the relative concentration and nature of defects on their surface changed depending on the conditions under which palladium was supported [48–50]. On the other hand, it is believed that, under conditions of UHV experiments, the rate of CO disproportionation is rather low and the products of CO dissociation can not always be detected. Indeed, in accordance with the results of theoretical calculations, the probability of CO dissociation on the surface of palladium is extremely low [53–55].

Adsorption of CO on the Defect Pd(111) Surface

Within the framework of this study, we examined the effect of surface defects on the dissociation of carbon monoxide in the course of CO adsorption on the defect surface of Pd(111). To prepare the defect surface, a precleaned sample was subjected to argon ion bombardment for an extended period (30 min; current density of 20 μA/cm^2) without subsequent annealing. In accordance with previous studies, the surface of a Pd(111) single crystal after argon etching consists of (111) terraces with great numbers of defects, such as steps, edges, and fractures [13, 15, 56]. Indeed, in this case, a noticeable blurring of the LEED image was observed; this fact provides support for the formation of a defect structure on the surface. As found previously, the crystal should be heated to 500–600 K in order to anneal induced defects [13, 15].

Figure 4 demonstrates the C 1*s* XPS and SFG spectra measured in the course of CO adsorption on atomically smooth and defect surfaces of a Pd(111) single crystal at 300 K. At a low pressure ($P_{CO} = 10^{-6}$ mbar), the SFG spectrum of the atomically smooth surface exhibited two lines at 1935 and 2075 cm^{-1}, which correspond to the stretching vibrations of CO molecules in bridging and terminal states, respectively. In this case, the C 1*s* XPS spectrum exhibited a line with $E_b = 285.6$ eV, which suggests the predominance of CO in a bridging form on the

surface [21, 37]. The formation of CO molecules adsorbed in a terminal form was detected by the appearance of an additional component with E_b = 286.2 eV, which manifested itself as a weakly pronounced shoulder on the side of higher binding energies in the C 1*s* spectrum.

In the case of the defect surface, the adsorption of CO resulted in the appearance of an additional SFG resonance in the region 1980–1992 cm^{-1} (Fig. 4a). At the same time, an increase in the relative intensity of the C 1*s* line by ~20% was observed; this suggests an increase in the specific surface area of the sample as a result of ion etching. An inadequate resolving power of the XPS spectrometer did not allow us to detect directly the appearance of additional C 1*s* components (Fig. 4b) in the case of CO adsorption on the defect surface of Pd(111). However, the use of a procedure of spectra subtraction (Fig. 4c) allowed us to detect spectroscopic differences in the XPS spectra. Thus, after subtracting the C 1*s* spectrum of the atomically smooth surface from the corresponding spectrum of the defect surface ($P_{CO} = 10^{-6}$ mbar), an additional C 1*s* state with E_b = 285.8 eV was clearly pronounced (Fig. 4c, spectrum *3–2*). At higher pressures, the terminal states are more populated and, accordingly, the difference spectrum shows a peak at ~286.2 eV (Fig. 4c, spectrum *4–3*).

Previously, in a study of CO adsorption on the supported palladium clusters $Pd/Al_2O_3/NiAl(110)$, it was found that CO molecules adsorbed in a bridging form on the (111) faces of palladium particles, as well as on the Pd(111) single-crystal surfaces, are characterized by the frequency of stretching vibrations ν(C–O) within the range 1910–1970 cm^{-1}. Higher vibrational frequencies (1970–2000 cm^{-1}) correspond to CO molecules adsorbed on defects such as the fractures and edges of palladium nanoclusters [13–15, 51–53]. Consequently, the SFG resonance observed in the region 1980–1992 cm^{-1}, as well as the additional C 1*s* state (E_b = 285.8 eV), belongs to CO molecules adsorbed in a bridging form at surface defects.

Unlike Matolín *et al.* [47], we did not detect CO dissociation traces on the defect surface of palladium. The adsorption of CO on both atomically smooth and defect surfaces of a Pd(111) single crystal was molecular even at elevated pressures. The accumulation of adsorbed carbon on the surface of palladium was not observed even after a long exposure at P_{CO} = 0.1 mbar and T = 400 K for several hours. The reason for the inconsistency of the above data with the published results [47] is unclear. It is likely that the previously observed effect of the formation of adsorbed carbon on the defect surface of palladium foil in the course of CO adsorption was due to the presence of carbonyl compounds in a gas phase [15, 21] or the segregation of carbon from the bulk of palladium [57].

The refutation of the defect-induced mechanism of CO dissociation [47] casts doubt on the hypothesis that carbon monoxide can also disproportionate on the surface of highly dispersed palladium particles [41–46]. It is most likely that the effect of trace impurities in the support and redistribution of these impurities in the course of catalyst preparation rather than particle size and the occurrence of specific defects play a crucial role in the dissociation of CO. The so-called strong metal–support interaction may also occur to result in the formation of intermetallic compounds at the metal–support interface. For example, in the case of Pt/TiO_2 catalysts, the formation of Pt_xTi fragments was assumed [58]. Indeed, the adsorption properties of the surfaces of Pt_3Ti polycrystals and single crystals and Pt/TiO_2 catalysts are significantly different from the properties of platinum monoliths [59]. It is believed that, in this case, the carbon atoms of adsorbed CO molecules interact with platinum atoms, which bear a small negative charge ($Pt^{\delta-}$), whereas the oxygen atoms react with positively charged $Ti^{\delta+}$ atoms. This state of adsorbed CO molecules is a predissociation state. An analogous model of the dissociative adsorption of CO was also proposed for a palladium–aluminum alloy [60]. It is likely that, in the course of preparation of $Pd/\gamma\text{-}Al_2O_3$ catalysts [46], the partial reduction of aluminum occurs with the formation of PdAl fragments. The adsorption of CO on these fragments results in a considerable weakening of the C–O bond in carbon monoxide molecules.

Methanol Decomposition on the Surface of Palladium

The inactivity of pure palladium in the dissociation of the C–O bond explains the activity of supported palladium catalysts in the synthesis of methanol [61]. A low contribution from the step of C–O bond cleavage, as compared with the steps of C–H and O–H bond formation, is responsible for the high selectivity of CO hydrogenation to methanol rather than methane on palladium, as in the case of a number of other metals (Co, Ni). At the same time, the formation of hydrogen-containing intermediates can accelerate the dissociation of the C–O bond and result in the buildup of carbon deposits on the surface of palladium, which causes catalyst deactivation. However, note that this reaction cannot be studied with the use of physical techniques because the synthesis of methanol takes place only at high pressures [61]. Therefore, many researchers studied the mechanism of a reverse reaction of methanol decomposition. Based on the principle of microscopic reversibility, it is believed that the reactions of CO hydrogenation to CH_3OH and methanol decomposition occur via the same intermediate steps.

Although the interaction of methanol with the surface of palladium was studied in detail by different teams of researchers, the mechanism of methanol decomposition is still an unsettled question [62–82]. The majority of authors are in agreement that the predominant path of this reaction is methanol dehydrogenation to CO and H_2 [62–71]. On the other hand, some authors have assumed the possibility of C–O bond

cleavage and the formation of adsorbed CH_x (x = 0–3) species [72–79]. Thus, the study of methanol adsorption on a polycrystalline palladium film at 120 and 300 K by ultraviolet photoelectron spectroscopy (UPS) allowed Lüth *et al.* [62] to find that, at a low temperature, methanol was molecularly adsorbed and bound to the metal surface through the lone electron pair of oxygen. At room temperature, methanol underwent decomposition with the formation of adsorbed CO and hydrogen. The studies of methanol decomposition on Pd(111) by secondary ion mass spectrometry (SIMS) [74] and electron-energy loss spectroscopy (EELS) [65] demonstrated that, at the first step, the decomposition of methanol occurred via O–H bond cleavage in the adsorbed methanol molecule with the formation of CH_3O groups. Upon subsequent heating, these groups decomposed to CO by stepwise elimination of hydrogen atoms with the formation of CH_2O_{ads} and CHO_{ads} intermediates. Analogous conclusions were also drawn based on the results obtained by TPD and EELS [70, 71].

Winograd and coauthors [72, 73], who used XPS, SIMS, and TPD techniques, were the first to assume the possibility of C–O bond dissociation in the methanol molecule upon adsorption on the surface of Pd(111). After the adsorption of methanol at 110 K ($\Theta \sim 0.5$ ML) followed by heating to 175 K in a vacuum, the formation of methyl fragments ($CH_{3,\,ads}$) with the concentration $\Theta = 0.04$ ML was observed on the Pd(111) surface. As the temperature was increased, CH_3 groups were further dehydrogenated to form $CH_{2,\,ads}$, CH_{ads}, and C_{ads} fragments. The accumulation of a small number of adsorbed CH_3 groups on the Pd(100) surface was also observed upon continuous supply of methanol at temperatures higher than 300 K [64]. On the other hand, the use of $^{13}CH_3{}^{16}OH$ and $^{12}CH_3{}^{18}OH$ isotope labels in a study of C–O bond activation in methanol on Pd(111) over a wide temperature range (87–265 K) did not allow Guo *et al.* [69] to detect the trace products of C–O bond cleavage in methanol using TPD with a sensitivity of ~0.01 ML.

To explain this contradiction, it was hypothesized [66, 80] that the activation of the C–O bond occurs only at specific defect sites, which also occur in small amounts on real single-crystal surfaces. This hypothesis was further supported by Schauermann *et al.* [78, 79], who found that the decomposition of methanol and the formation of CH_x fragments occur with a high efficiency on the supported palladium clusters $Pd/Al_2O_3/NiAl(110)$ at temperatures higher than 300 K. However, in our opinion, differences in the kinetics of various reaction paths in methanol decomposition on the surface of palladium may be responsible for contradictory experimental data. Because the rate of methanol dehydrogenation to CO is higher than the rate of methanol decomposition with C–O bond cleavage by about two orders of magnitude [79], it is practically impossible to detect the formation of $CH_{x,\,ads}$ fragments in UHV experiments (low temperatures and low methanol exposures).

To test our hypothesis, in this work we used XPS and SFG spectroscopy for studying the interaction of methanol with the atomically smooth Pd(111) surface on varying temperature and pressure. Figure 5 shows the SFG and C 1*s* XPS spectra obtained *in situ* in the course of methanol decomposition on the Pd(111) surface at 300 and 400 K. As can be seen, the adsorption of methanol at 10^{-6} mbar and room temperature resulted in the appearance of a resonance in the SFG spectra with a vibration frequency of 1915 cm^{-1}, which corresponds to adsorbed CO molecules in bridging from with $\Theta \sim 0.5$ ML [15, 21, 30–35, 38]. In this case, the C 1*s* spectrum exhibited two components with binding energies of ~284 and 285.6 eV. In accordance with published data [21, 36, 39], the former line can be attributed to $CH_{x,\,ads}$ (x = 0–3) hydrocarbon species, whereas the latter can be ascribed to oxygen-containing fragments like CH_xO_{ads} (x = 0–3). However, the quantitative agreement between the coverage ($\Theta \sim 0.5$ ML) determined from the relative intensity of the C 1*s* signal with E_b = 285.6 eV and SFG data allowed us to narrow the range of conceivable candidates and to attribute this signal to adsorbed CO. This assignment was supported by the results of many EELS studies; it was found that the decomposition of CH_3O groups to CO_{ads} on the surface of palladium occurred even at 200–250 K [65, 68, 71]. The intensity of the first component of the C 1*s* spectrum continuously increased with time, whereas the surface concentration of CO remained practically unchanged (Table 2, Fig. 6).

An increase in the temperature to 400 K or in the pressure to 0.1 mbar resulted in a dramatic increase in the surface concentration of CH_x species (Fig. 5). Thus, at 300 K and P_{MeOH} = 0.1 mbar, the C 1*s* line intensity (E_b = 283.8 eV) corresponds to $\Theta \sim 1.0$ ML (Table 2). In spite of these high coverages, a portion of the surface was covered with adsorbed CO molecules with $\Theta \sim 0.4$–0.5 ML (Fig. 5, Table 2). The excess of the total amount of adsorbed species (both CH_x and CO) over a monolayer coverage can be explained by either the dissolution of a portion of carbon in the near-surface region of palladium [83] or the formation of three-dimensional carbon structures. At 400 K and P = 0.1 mbar, the amount of carbon additionally increased ($\Theta \sim 1.5$ ML), and a slight shift of this C 1*s* component to higher binding energies (E_b = 284.0 eV) was observed. This may represent a manifestation of the above transformations of carbon deposits. The C 1*s* line at 288 eV is due to gas-phase methanol.

Thus, the above results unambiguously demonstrate that the activation of the C–O bond in methanol also occurs at a detectable rate on the atomically smooth Pd(111) surface at 300–400 K. The rate of decomposition of methanol and the rate of formation of adsorbed carbon increased with pressure and temperature. The resulting carbon caused the carbonization and complete

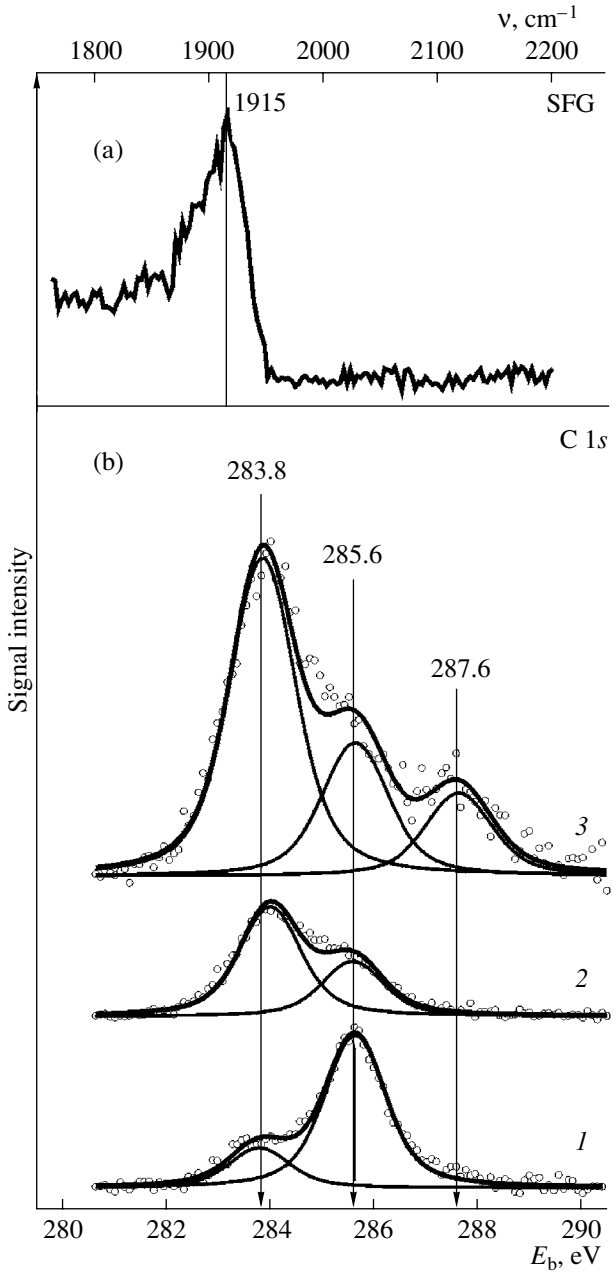

Fig. 5. (a) SFG spectrum recorded *in situ* at T = 300 K and $P_{CH_3OH} = 10^{-6}$ mbar; (b) C 1*s* XPS spectra recorded *in situ* in the course of methanol decomposition on the atomically smooth surface Pd(111): (*1*) $P = 10^{-6}$ mbar, T = 300 K; (*2*) $P = 10^{-6}$ mbar, T = 400 K; and (*3*) P = 0.1 mbar, T = 300 K.

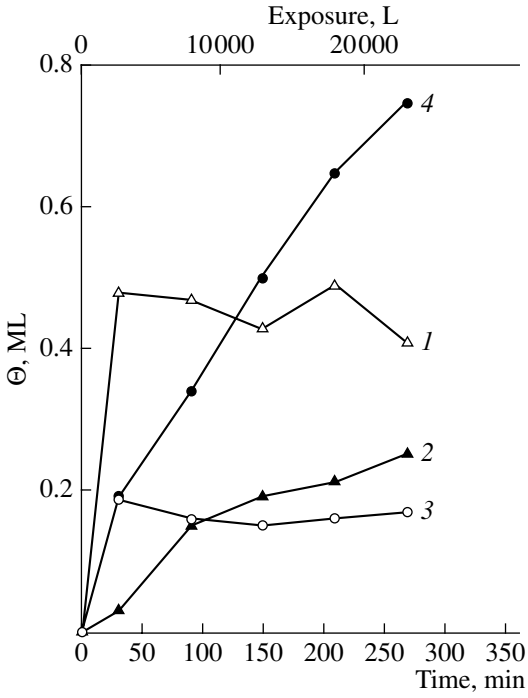

Fig. 6. Changes in the surface concentrations of (*1*, *3*) CO and (*2*, *4*) CH_x species formed on the atomically smooth surface Pd(111) in the course of methanol decomposition at $P = 10^{-6}$ mbar and T= (*1*, *2*) 300 and (*3*, *4*) 400 K. The exposure of CH_3OH is expressed in langmuir units (1 L = 10^{-6} Torr s).

deactivation of the surface. Even at elevated pressures (15–30 mbar of methanol in an atmosphere of helium), we failed to detect the buildup of methanol decomposition products on Pd(111) at 300–600 K for several hours using gas chromatography. However, on the addition of oxygen to the reaction mixture, a rapid oxidation of methanol to CO_2 and H_2O was observed. The decomposition of methanol is not a structure-sensitive reaction, and it occurs at approximately equal rates on both atomically smooth and defect Pd(111) surfaces [10]. The decomposition of methanol on the surface of Pd(111) was considered in more detail in [77].

Mechanism of C–O Bond Activation on the Surface of Palladium

The donor–acceptor model proposed by Blyholder [84] is most frequently used for describing the interaction of adsorbed CO molecules with transition-metal surfaces. According to this model, the CO molecule is bound to the metal surface via the carbon atom, and the molecular axis is oriented perpendicularly to the surface. The chemisorption M–CO bond is formed because of electron-density transfer from the 5σ molecular orbital of CO to unoccupied *d* orbitals of the metal. A reverse donation of electrons from the occupied *d* orbitals of the metal to the unoccupied 2π* orbital of CO is observed simultaneously. The 4σ and 1π molecular orbitals of the CO molecule are bonding orbitals, and they practically do not participate in the formation of M–CO bonds. The Blyholder model was theoretically substantiated in [85, 86]. The M–CO donor–acceptor interaction in a wide range of transition metals was supported experimentally by UPS [87].

Table 2. Changes in the surface concentrations of CO and $CH_{x,\,ads}$ (Θ, ML) during the adsorption of CH_3OH on the atomically smooth surface Pd(111) at 300 and 400 K

Experimental conditions	Time, min					Surface species
	30	90	150	210	270	
$P_{CH_3OH} = 10^{-6}$ mbar, $T = 300$ K	0.03	0.15	0.19	0.21	0.26	CH_x
	0.48	0.47	0.47	0.47	0.43	CO
$P_{CH_3OH} = 10^{-6}$ mbar, $T = 400$ K	0.17	0.33	0.48	0.62	0.74	CH_x
	0.19	0.17	0.16	0.17	0.17	CO
$P_{CH_3OH} = 0.1$ mbar, $T = 300$ K	1.0	0.97	1.0	0.93	–	CH_x
	0.50	0.48	0.41	0.37	–	CO

In terms of this model, the mechanism of C–O bond activation was studied. It was found that electron-density transfer from the 5σ orbital of CO to unoccupied orbitals of the metal had almost no effect on the strength of the C–O bond, whereas the reverse donation of electrons from the *d* orbitals of the metal to the antibonding 2π* orbital of CO resulted in its destabilization. It was demonstrated that the activation energy of C–O bond dissociation correlates with the occupancy of the antibonding 2π* orbital [7, 87].

The geometric structure of an adsorption complex is also considered among factors responsible for the probability of C–O dissociation on the surfaces of transition metals. It is believed that the C–O bond is activated because of the formation of a predissociative state, in which both the carbon atom and the oxygen atom of the CO molecule are chemically bound to the surface [7, 88]. It was found that, at 120 K, the adsorption of CO on the Cr(110) surface at low coverages ($\Theta < 0.25$ ML) resulted in the formation of the $c(4 \times 2)$ structure, in which the CO molecules are oriented parallel to the surface [89, 90]. This state of adsorbed carbon monoxide is characterized by an unusually low frequency of stretching vibrations ν(C–O) in the range 1150–1330 cm^{-1}, which is indicative of a considerable weakening of the C–O bond. On heating to 200 K, the dissociation of CO was observed. In a study of CO adsorption on the Fe(100) surface by X-ray absorption, an adsorption species with the CO molecule inclined at an angle of 45° ± 10° to the surface was detected [91, 92]. According to Moon and coauthors [91, 92], this state is also a precursor of CO dissociation. Of course, electron and geometry factors are interrelated in the activation of the C–O bond. In the predissociative state, in which the molecular axis of CO is considerably deflected from a normal to the surface, the hybridization of the 2π* orbital of CO with the *d* orbitals of the metal and, correspondingly, a weakening of the C–O bond occurred.

The formation of adsorption complexes, in which the molecular axis of CO is deflected with respect to a normal to the surface, was detected in the majority of transition metals. As a consequence, the following reaction of carbon monoxide disproportionation (Boudart reaction) occurs on the surfaces of many transition metals at elevated temperatures [7]:

$$CO + CO \longrightarrow C_{ads} + CO_2.$$

In the case of palladium, adsorbed carbon monoxide molecules are oriented perpendicularly to the surface. Note that this structure of the adsorption complex was found in both the closely packed face Pd(111) and the stepped faces Pd(112) and Pd(311) [93–95]. Consequently, the dissociation of CO on the pure surface of palladium is improbable. In full agreement with the above statement, we did not detect dissociation traces in the course of carbon monoxide adsorption on atomically smooth and defect Pd(111) surfaces over wide ranges of temperatures (200–400 K) and pressures (10^{-6}–1 mbar).

Another mechanism of C–O bond activation should take place in the case of methanol adsorption. Indeed, in the course of methanol dehydrogenation, the geometric structure of the adsorption complex was dramatically changed. Figure 7 shows the conceivable steps of the molecular transformation of methanol in the course of dehydrogenation to CO by the reaction

$$CH_3OH \longrightarrow CO + 2H_2.$$

In accordance with experimental data, the initial step of methanol decomposition is the cleavage of the O–H bond and the formation of CH_3O_{ads} [65, 67–71]. Methoxy groups, as well as adsorbed methanol molecules, are bound to the surface of palladium through the lone electron pair of the oxygen atom and oriented almost perpendicularly to the surface [62]. In the course of further dehydrogenation, the molecular axis of the adsorbed complex turned through 90°, so that formaldehyde (CH_2O_{ads}) and formyl (CHO_{ads}) were oriented parallel to the surface of palladium [80–82]. As mentioned above, the final product of dehydrogenation (the CO molecule) was oriented perpendicularly to the surface and bound to metal atoms through the carbon atom [93–95]. The occurrence of CH_xO ($x = 1$–2) adsorption complexes oriented parallel to the surface of palladium

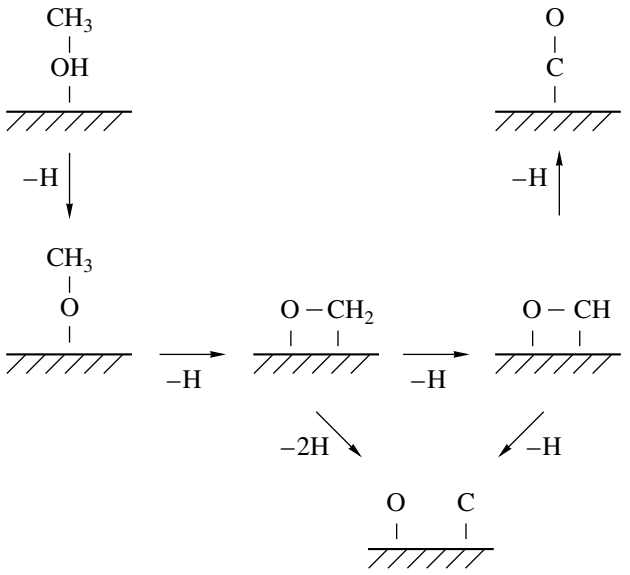

Fig. 7. Model of methanol decomposition on the surface of palladium.

suggests that they can be considered as predissociation states that result in C–O bond cleavage (see Fig. 7).

The formation of carbon deposits on the atomically smooth surface Pd(111) that was detected in this work (Fig. 5), provides support for the validity of the mechanism of C–O bond activation in the interaction of methanol with the surface of palladium (Fig. 7 illustrates this mechanism). Evidently, an increase in the lifetime of reaction intermediates of methanol dehydrogenation will result in a higher probability of C–O bond dissociation. It is likely that this circumstance can also explain the observed increase in the rate of carbon buildup at high pressures (Fig. 5) in the case of defect sites on the surface of supported palladium clusters [78, 79].

Taking into account the principle of microreversibility, we assume that C–O bond dissociation and catalyst deactivation due to the accumulation of carbon deposits can also occur in the case of the reaction of CO hydrogenation on palladium

$$CO + 2H_2 \longrightarrow CH_3OH.$$

Indeed, we previously detected the appearance of a corresponding C 1*s* signal (E_b ~284 eV) in the XPS spectra measured *in situ* in the course of the interaction of CO + H_2 mixtures with the surface Pd(111) [96].

CONCLUSIONS

We studied the adsorption of CO on atomically smooth and defect Pd(111) surfaces using SFG and XPS techniques over the temperature range 200–400 K and the pressure range 10^{-6}–1 mbar. We found that carbon monoxide was adsorbed as surface forms such as threefold hollow, bridging, and terminal species, even at high pressures. High pressures allowed us to reach higher equilibrium coverages, particularly in the case of the most weakly bound terminal state of CO. We have not found any evidence for the dissociation of CO or the formation of carbonyls on clean palladium surfaces under conditions of our experiments, although it has been hypothesized in the last few years that this can occur at elevated pressures.

In contrast to CO, the character of methanol adsorption on Pd(111) depends on pressure. Along with the well-known reaction path of CH_3OH decomposition to CO and hydrogen, which was identified previously in many UHV experiments, the contribution of the slow process of methanol decomposition to elemental carbon increases at high pressures. Finally, the formation of carbon results in the complete deactivation of the surface.

The experimental data are explained in terms of the Blyholder model, which describes the interaction of CO with transition metal surfaces with the use of electron-density transfer between the *d* orbitals of the metal and the $5\sigma/2\pi^*$ molecular orbitals of CO. It is hypothesized that the geometry of the adsorption complex is a key factor in this interaction (particularly in the reverse donation of electrons from the metal to the $2\pi^*$ antibonding orbital, which facilitates the dissociation of the C–O bond). In the case of adsorbed CO, the perpendicular arrangement of the molecular axis decreases the contribution of the reverse donation; consequently, it is responsible for the inactivity of palladium in C–O bond dissociation. In the case of methanol dehydrogenation (or CO hydrogenation), the formation of intermediates such as CH_xO ($x = 1$ or 2), whose axes are arranged parallel to the surface of palladium, facilitates electron transfer form the metal to the $2\pi^*$ antibonding orbital of CO to weaken the strength of the C–O bond. Finally, this results in the dissociation of this bond and in the blocking of the palladium surface by carbon deposits.

ACKNOWLEDGMENTS

We are grateful to I.P. Prosvirin, M. Morkel, H. Unterhalt, and M. Borasio for their experimental assistance and valuable discussions of the results of this study. Kaichev thanks the Max Planck Society and DAAD for the financial support of scientific probation at the Fritz Haber Institute. Bukhtiyarov acknowledges the Russian Science Support Foundation (a grant for young Doctors of Science).

REFERENCES

1. Vannice, M.A., *J. Catal.*, 1975, vol. 37, pp. 449, 462.
2. Biloen, P. and Sachtler, W.M.H., *Adv. Catal.*, 1981, vol. 30, p. 165.
3. Bell, A.T., *Catal. Rev.*, 1981, vol. 23, p. 203.
4. Henrici-Olive, G. and Olive, S., *The Chemistry of the Catalyzed Hydrogenation of Carbon Monoxide*, Berlin: Springer, 1984.

5. Anderson, R.B., *The Fischer–Tropsch Synthesis*, London: Academic, 1984.
6. Slivinskii, E.V. and Voitsekhovskii, Yu.P., *Usp. Khim.*, 1989, vol. 58, p. 94.
7. Hindermann, J.P., Hutchings, G.J., and Kiennemann, A., *Catal. Rev.*, 1993, vol. 35, p. 1.
8. Szanyi, J., Kuhn, W.K., and Goodman, D.W., *J. Vac. Sci. Technol., A*, 1993, vol. 11, p. 1969.
9. Ozensoy, E., Meier, D.C., and Goodman, D.W., *J. Phys. Chem. B*, 2002, vol. 106, p. 9367.
10. Rodriguez de la Fuente, O., Borasio, M., Galletto, P., Rupprechter, G., and Freund, H.-J., *Surf. Sci.*, 2004, vols. 566–568, p. 740.
11. Cremer, P.S., McIntyre, B.J., Salmeron, M., Shen, Y.-R., and Somorjai, G.A., *Catal. Lett.*, 1995, vol. 34, p. 11.
12. Somorjai, G.A. and Rupprechter, G., *J. Phys. Chem. B*, 1999, vol. 103, p. 1623.
13. Rupprechter, G., Dellwig, T., Unterhalt, H., and Freund, H.-J., *J. Phys. Chem. B*, 2001, vol. 105, p. 3797.
14. Rupprechter, G., *Phys. Chem. Chem. Phys.*, 2001, vol. 3, p. 4621.
15. Rupprechter, G., Unterhalt, H., Morkel, M., Galletto, P., Hu, L., and Freund, H.-J., *Surf. Sci.*, 2002, vol. 502, p. 109.
16. Knop-Gericke, A., Hävecker, M., Shedel-Niedrig, Th., and Schlögl, R., *Top. Catal.*, 2001, vol. 15, p. 27.
17. Bukhtiyarov, V.I., Hävecker, M., Kaichev, V.V., Knop-Gericke, A., Mayer, R.W., and Schlögl, R., *Catal. Lett.*, 2001, vol. 74, p. 121.
18. Bluhm, H., Hävecker, M., Kleimenov, E., Knop-Gericke, A., Liskowski, A., Schlögl, R., and Su, D.S., *Top. Catal.*, 2003, vol. 23, p. 99.
19. Joyner, R.W., Roberts, M.W., and Yates, K., *Surf. Sci.*, 1979, vol. 87, p. 501.
20. Prosvirin, I.P., Tikhomirov, E.P., Sorokin, A.M., Kaichev, V.V., and Bukhtiyarov, V.I., *Kinet. Katal.*, 2003, vol. 44, no. 5, p. 724.
21. Kaichev, V.V., Prosvirin, I.P., Bukhtiyarov, V.I., Unterhalt, H., Rupprechter, G., and Freund, H.-J., *J. Phys. Chem. B*, 2003, vol. 107, p. 3522.
22. Bukhtiyarov, V.I., Kaichev, V.V., and Prosvirin, I.P., *Top. Catal.*, 2005, vol. 32, p. 3.
23. Hunt, J.H., Guyot-Sionnest, P., and Shen, Y.R., *Chem. Phys. Lett.*, 1987, vol. 133, p. 189.
24. Shen, Y.R., *Nature*, 1989, vol. 337, p. 519.
25. Shen, Y.R., *Surf. Sci.*, 1994, vols. 299–300, p. 551.
26. Liang, D.B., Abend, G., Block, J.H., and Kruse, N., *Surf. Sci.*, 1983, vol. 126, p. 392.
27. Mihaylov, M., Hadjiivanov, K., and Knözinger, H., *Catal. Lett.*, 2001, vol. 76, p. 59.
28. Kishi, K., Motoyoshi, Y., and Ikeda, S., *Surf. Sci.*, 1981, vol. 105, p. 313.
29. Engel, T., *J. Chem. Phys.*, 1978, vol. 69, p. 373.
30. Bradshaw, A.M. and Hoffmann, F.M., *Surf. Sci.*, 1978, vol. 72, p. 513.
31. Hoffmann, F.M., *Surf. Sci. Rep.*, 1983, vol. 3, p. 107.
32. Guo, X. and Yates, T., Jr, *J. Chem. Phys.*, 1989, vol. 90, p. 6761.
33. Tüshaus, M., Berndt, W., Conrad, H., Bradshow, A.M., and Persson, B., *Appl. Phys. A*, 1990, vol. 51, p. 91.
34. Szanyi, J., Kuhn, W.K., and Goodman, D.W., *J. Phys. Chem.*, 1994, vol. 98, p. 2978.
35. Bourguignon, B., Carrez, S., Dragnea, B., and Dubost, H., *Surf. Sci.*, 1998, vol. 418, p. 171.
36. Surnev, S., Sock, M., Ramsey, M.G., Netzer, F.P., Wiklund, M., Borg, M., and Anderson, J.N., *Surf. Sci.*, 2000, vol. 470, p. 171.
37. Kaichev, V.V., Morkel, M., Unterhalt, H., Prosvirin, I.P., Bukhtiyarov, V.I., Rupprechter, G., and Freund, H.-J., *Surf. Sci.*, 2004, vols. 566–568, p. 1024.
38. Morkel, M., Rupprechter, G., and Freund, H.-J., *J. Chem. Phys.*, 2003, vol. 119, p. 10853.
39. Rodriguez, N.M., Anderson, P.E., Wootsch, A., Wild, U., Schlögl, R., and Paal, Z., *J. Catal.*, 2001, vol. 197, p. 365.
40. Barber, M., Connor, J.A., Guest, M.F., Hall, M.B., Hillier, I.H., and Meredith, W.N.E., *Faraday Discuss. Chem. Soc.*, 1972, vol. 54, p. 219.
41. Doering, D.L., Poppa, H., and Dickinson, J.T., *J. Catal.*, 1982, vol. 73, p. 104.
42. Ichikawa, S., Poppa, H., and Boudart, M., *J. Catal.*, 1985, vol. 91, p. 1.
43. Dropsch, H. and Baerns, M., *Appl. Catal., A*, 1997, vol. 158, p. 163.
44. Matolín, V., Gillet, E., and Kruse, N., *Surf. Sci.*, 1987, vol. 186, p. L541.
45. Matolín, V. and Gillet, E., *Surf. Sci.*, 1990, vol. 238, p. 75.
46. Stará, I. and Matolín, V., *Surf. Sci.*, 1994, vol. 313, p. 99.
47. Matolín, V., Rebholz, M., and Kruse, N., *Surf. Sci.*, 1991, vol. 245, p. 233.
48. Koch, R. and Poppa, H., *J. Vac. Sci. Technol., A*, 1987, vol. 5, p. 1845.
49. Henry, C.R., Chapon, C., Goyhenex, C., and Monot, R., *Surf. Sci.*, 1992, vol. 272, p. 283.
50. Cordatos, H., Bunluesin, T., and Gorte, R.J., *Surf. Sci.*, 1995, vol. 323, p. 219.
51. Wolter, K., Seiferth, O., Kunlenbeck, H., Bäumer, M., and Freund, H.-J., *Surf. Sci.*, 1998, vol. 399, p. 190.
52. Bäumer, M. and Freund, H.-J., *Prog. Surf. Sci.*, 1999, vol. 61, p. 127.
53. Yudanov, I.V., Sahnoun, R., Neyman, K.M., Rösch, N., Hoffmann, J., Schauermann, S., Johánek, V., Unterhalt, H., Rupprechter, G., Libuda, J., and Freund, H.-J., *J. Phys. Chem. B*, 2003, vol. 107, p. 255.
54. Shustorovich, E. and Bell, A.T., *Surf. Sci.*, 1991, vol. 253, p. 386.
55. Neurock, M., *Top. Catal.*, 1999, vol. 9, p. 135.
56. Rodriguez, O., Gonzalez, M.A., and Rojo, J.M., *Phys. Rev. B: Condens. Matter*, 2001, vol. 63, p. 085420.
57. Ratajczykowa, I., *J. Vac. Sci. Technol., A*, 1983, vol. 1, p. 1512.
58. Tauster, S.J., Fung, S.C., and Garten, R.L., *J. Am. Chem. Soc.*, 1978, vol. 100, p. 170.
59. Mehandru, S.P., Anderson, A.B., and Ross, P.N., *J. Catal.*, 1986, vol. 100, p. 210.
60. Johánek, V., Stará, I., and Matolín, V., *Surf. Sci.*, 2002, vol. 507, p. 92.

61. Poutsma, M.L., Elek, L.F., Ibarbia, P.A., Risch, A.P., and Rabo, J.A., *J. Catal.*, 1978, vol. 52, p. 157.
62. Lüth, H., Rubloff, G.W., and Grobmann, W.D., *Surf. Sci.*, 1977, vol. 63, p. 325.
63. Christmann, K. and Demuth, J.E., *J. Chem. Phys.*, 1982, vol. 76, pp. 6308, 6318.
64. Solymosi, F., Berkó, A., and Tóth, Z., *Surf. Sci.*, 1993, vol. 285, p. 197.
65. Bhattacharya, A.K., Chesters, M.A., Pemble, M.E., and Sheppard, N., *Surf. Sci.*, 1988, vol. 206, p. L845.
66. Hartmann, N., Esch, F., and Imbihl, R., *Science*, 1993, vol. 297, p. 175.
67. Kok, G.A., Noordermeer, A., and Nieuwenhuys, B.E., *Surf. Sci.*, 1983, vol. 135, p. 65.
68. Gates, J.A. and Kesmodel, L.L., *J. Catal.*, 1983, vol. 83, p. 437.
69. Guo, X., Hanley, L., and Yates, J.T., Jr., *J. Am. Chem. Soc.*, 1989, vol. 111, p. 3155.
70. Davis, J.L. and Bareau, M.A., *Surf. Sci.*, 1987, vol. 187, p. 387.
71. Davis, J.L. and Bareau, M.A., *Surf. Sci.*, 1990, vol. 235, p. 235.
72. Levis, R.J., Zhicheng, J., and Winograd, N., *J. Am. Chem. Soc.*, 1989, vol. 111, p. 4605.
73. Chen, J.-J., Jaing, Z.-C., Zhou, Y., Chakraborty, B.R., and Winograd, N., *Surf. Sci.*, 1995, vol. 328, p. 248.
74. Rebholz, M., Matolín, V., Prins, R., and Kruse, N., *Surf. Sci.*, 1991, vol. 251, p. 1117.
75. Kruse, N., Rebholz, M., Matolín, V., Chuah, G.K., and Block, J.H., *Surf. Sci.*, 1990, vol. 238, p. L457.
76. Rebholz, M. and Kruse, N., *J. Chem. Phys.*, 1991, vol. 95, p. 7745.
77. Morkel, M., Kaichev, V.V., Borasio, M., Rupprechter, G., Freund, H.-J., Prosvirin, I.P., and Bukhtiyarov, V.I., *J. Phys. Chem. B*, 2004, vol. 108, p. 12955.
78. Schauermann, S., Hoffmann, J., Johánek, V., Hartmann, J., Libuda, J., and Freund, H.-J., *Angew. Chem., Int. Ed. Engl.*, 2002, vol. 41, p. 2532.
79. Schauermann, S., Hoffmann, J., Johanek, V., Hartmann, J., Libuda, J., and Freund, H.-J., *Catal. Lett.*, 2002, vol. 84, p. 209.
80. Mavrikakis, M. and Barteau, M.A., *J. Mol. Catal. A*, 1998, vol. 131, p. 135.
81. Zhang, C.J. and Hu, P., *J. Chem. Phys.*, 2001, vol. 115, p. 7182.
82. Desai, S.K., Neurock, M., and Kourtakis, K., *J. Phys. Chem. B*, 2002, vol. 106, p. 2559.
83. Yudanov, I.V., Neyman, K.M., and Rösch, N., *Phys. Chem. Chem. Phys.*, 2004, vol. 6, p. 116.
84. Blyholder, G., *J. Phys. Chem.*, 1964, vol. 68, p. 2772.
85. Doyen, G. and Ertl, G., *Surf. Sci.*, 1977, vol. 69, p. 157.
86. Rosen, A., Grundevik, P., and Moravic, T., *Surf. Sci.*, 1980, vol. 95, p. 477.
87. Broden, G., Rhodin, T.N., Bruckner, C.F., Benbow, R., and Hurych, Z., *Surf. Sci.*, 1976, vol. 59, p. 593.
88. Ponec, V., *Catal. Rev.*, 1978, vol. 18, p. 151.
89. Shinn, N.D. and Madey, T.E., *J. Vac. Sci. Technol., A*, 1985, vol. 3, p. 1673.
90. Shinn, N.D. and Madey, T.E., *J. Chem. Phys.*, 1985, vol. 83, p. 5928.
91. Moon, D.W., Bernasek, S.L., Dwyer, D.J., and Gland, J.L., *J. Am. Chem. Soc.*, 1985, vol. 107, p. 4363.
92. Moon, D.W., Cameron, S., Zaera, F., Eberhardt, W., Carr, R., Bernasek, S.L., Gland, J.L., and Dwyer, D.J., *Surf. Sci.*, 1987, vol. 180, p. L123.
93. Ramsier, R.D., Lee, K.-W., and Yates, J.T., Jr., *Surf. Sci.*, 1995, vol. 322, p. 243.
94. Schilbe, P., Farias, D., and Rieder, K.H., *Chem. Phys. Lett.*, 1997, vol. 281, p. 366.
95. Galletto, P., Unterhalt, H., and Rupprechter, G., *Chem. Phys. Lett.*, 2003, vol. 367, p. 785.
96. Rupprechter, G., Kaichev, V.V., Unterhalt, H., Morkel, M., and Bukhtiyarov, V.I., *Vacuum* (in press).